Large Electric Load Fluctuations in Energy-Efficient Buildings and how to Suppress them with Demand Side Management

Tommaso Coletta, Robin Delabays, Laurent Pagnier, and Philippe Jacquod

***Abstract*—Demand side management (DSM) is known for generating synchronized behaviors of aggregated loads that can lead to large, often long-term power fluctuations and even system instabilities. In contrast to this well-studied occurrence, we report here on the emergence of novel synchronized behaviors of thermostatically-controlled electric heating systems in buildings with good thermal insulation and important solar radiation gains without DSM. Synchrony of more than 80% of aggregated heating systems may arise during sunny and cold winter days in countries with temperate climate and energy-efficient buildings. To suppress the resulting large load fluctuations on the distribution grid we propose a centralized DSM algorithm that smoothens the total load curve – including electric heating and all other domestic appliances – of the cluster of dwellings it pilots. Setting up the baseline load is based on weather forecasts for a receding time-horizon covering the next 24 hours, while control actions are based on a priority list which is constructed from the current status of the dwellings. We show numerically that our DSM control scheme can be generically used to modify load curves of domestic households to achieve diverse goals such as minimizing electricity costs, peak shaving and valley filling.**

***Index Terms*—Demand side management, thermostatically controllable loads, direct load control, residual load**

I. Introduction.

Many western countries are now firmly engaged in the energy transition whose utimate goal is to meet energy demand from human activities solely with renewable sources. In its current intermediate stages, the transition steadily increases the penetration of nondispatchable electricity productions, which results in large uncontrolled fluctuations in power generation. Enforcing the balance between power demand and production under these circumstances becomes a challenge, which one standardly tries to meet with electrical energy storage. An alternative to storage is demand side management (DSM) where consumption is modified to balance production. Today DSM attempts to reach very diverse goals such as peak shaving and load shifting, financial optimization, self-consumption or providing ancillary services such as regulation reserves as well as frequency or voltage control [1] .

In parallel to changes in production, the energy transition aims at making human activities more energy-efficient. Buildings and households are one of the main targets of these efforts as they typically represent between 30 and 40% of the total energy consumption in western countries. Directives are therefore issued to construct new energy-efficient buildings with significantly better thermal insulation and increased solar radiation gains, and to renovate old ones along the same lines. Energy-efficiency is also improved via increased electrification of heating and cooling. This generates new opportunities for DSM, because thermostatically controlled loads (TCL) such as electric heaters, AC coolers and water boilers are characterized by a significant usage flexibility [2]. As a matter of fact, buildings have a sizeable thermal inertia that allows to delay or anticipate electric heating operation. Anticipated operation allows to store electric power as thermal energy, while delayed operation releases part of that thermal energy back into the grid in the form of reduced power demand. A variety of DSM schemes based on TCL have been proposed for minimizing electricity costs [3], to provide active power reserves [4], [5], [6] or ancillary services such as primary voltage control [7] and primary frequency control [8], [9], [10].

Quite unexpectedly, electric heating systems in energy-efficient buildings submitted to more or less homogeneous weather conditions can undergo a synchronization transition to a state where a large fraction of them switches on and off in unison – a fact that has not been recognized so far. Fig. 1 shows the aggregated electric heating load of a collection of 1000 energy-efficient individual houses. Atmospheric conditions – external temperature and solar radiation shown in Panel a) – are similar for all houses and obtained from a historical time series corresponding to one sunny winter week in January in the city of Sion, Switzerland. Details of the calculation are discussed below. During the second half of the week the weather is clear [solar radiation data are shown in blue in panel a)], solar heat gains through windows are important and contribute significantly to the heating of the buildings. One sees in panel b) that this leads to the switching off of most of the heating systems at around noon. Solar gains next vanish as the sun sets, which leads to the coherent switching on of most heating systems. We have found that this synchronous operation persists over periods of sunny weather (see below) and is damped only after few consecutive days with reduced solar radiation. It arises systematically in energy-efficient buildings with large solar energy gains and good thermal insulation, during sunny winter days. Fig. 1 c) further shows that oscillations clearly affect the total load, obtained by summing the consumptions of the electric heating and of the domestic appliances. Because they are dephased with respect to solar radiation, these oscillations cannot be directly compensated by local photovoltaic productions. One

The authors are with the School of Engineering of the University of Applied Sciences of Western Switzerland HES-SO, CH-1951 Sion, Switzerland (email: tommaso.coletta@hevs.ch (corresponding author); robin.delabays@hevs.ch; laurent.pagnier@hevs.ch; philippe.jacquod@hevs.ch)

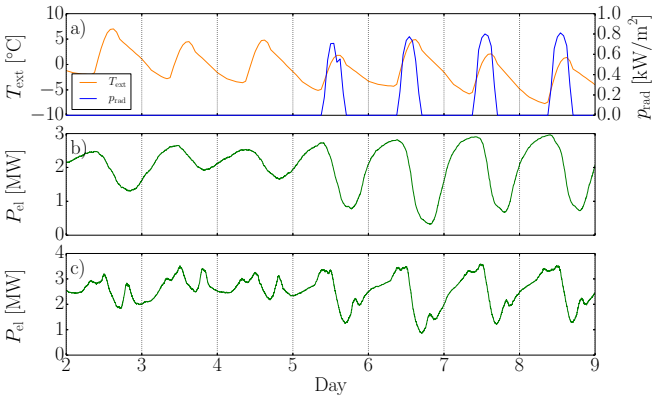

Fig. 1. Uncontrolled operation of 1000 aggregated households over one typical winter week in the city of Sion, Switzerland. Panel a): temperature (orange) and solar radiation (blue) data. Panel b): load of the electric heating systems (heat pumps with COP=3). Panel c): total load, including heating systems and domestic appliances. Vertical dotted lines indicate midnight.

unwanted, and so far overlooked consequence of the energy transition is thus that increasing energy efficiency in buildings eventually leads to a synchronous behavior of large sets of electric heating systems that may hamper the operation of electric power distribution systems. It is one of our main purposes here to illustrate how DSM coordination can smooth these large load oscillations.

In this manuscript, we propose a centralized DSM coordination scheme for non-disruptive peak shaving and valley filling of the load curve of aggregated households. By non-disruptive, we mean with no significant impact on end-use performance, that is without causing violations of the comfort temperature windows set by the end users, nor generating frequent switching on and off of the electric heating systems, nor increasing the total electric consumption. Our method is based on a new concept which we call *residual consumption*, and which in the present context refers to the sum of all non-flexible consumptions (mostly those of domestic appliances) from which non-flexible delocalized productions (mostly photovoltaics) are subtracted. Clearly, the residual consumption measures the amount of electricity that the considered group of households has to request from its electricity provider at a given time. Our aim is therefore to predict moments of high and low residual consumption in a time window spanning, for instance, the next 24 hours.

Then, in order to provide a service to the distribution system operator (DSO) by smoothing the overall load curve, the flexible electric heating systems are turned on at times of lesser residual consumption and turned off when it is larger. This is done by piloting the loads to try and match a predicted optimal load curve. The latter is obtained by estimating future heating needs from weather forecasts, as well as predictions on non-flexible consumption or future evolutions of electricity prices.

The paper is organized as follows: Section II describes the model used to account for heat exchanges and temperature control in buildings. Section III presents the underlying principles of our control scheme and compares it to conventional thermostat regulation. The details of the implementation of our control algorithm are given in Section IV while the simulation parameters and the results obtained are presented in Section V. A brief conclusion is given in Section VI.

II. Electric Heating Modeling

We consider a simplified, yet standard model for thermostatically-constrained electric heating [11], [12]. The state of each building is described by a single average internal temperature T whose time-evolution is governed by the following differential equation,

$$C\,\frac{dT}{dt} = \kappa\;[T_{\rm ext}(t) - T] + P_{\rm h}(t) + P_{\rm rad}(t)\,. \qquad (1)$$

The left-hand side gives the change in energy stored in the building's thermal mass as its temperature changes. The constant C [Wh/K] depends on the volume and the material used for the building's walls, floors and so forth. It represents a thermal inertia, with the internal temperature varying more easily if C is small. The first term on the right-hand side represents the heat exchange with the exterior, with the effective thermal conductivity κ [W/K] being determined by the building's insulation (including windows, doors and walls). Energy-efficient buildings are well insulated, which manifests itself in a smaller κ. The heat exchange term is proportional to the difference between the external and internal temperatures, with the sign of this difference determining whether heat flows from the building to the exterior or vice-versa. The last two terms on the right hand side of (1), are respectively the power input $P_{\rm h}$ [W] of the heating system and the solar radiation gain $P_{\rm rad}$ [W]. The latter is obtained by multiplying the meteorological solar radiation data on a vertical surface, by the window surface S and a transmission coefficient g,

$$P_{\rm rad}(t) = p_{\rm rad}(t)\;S\;\;g\,. \qquad (2)$$

The transmission coefficient $g \in [0,1]$, with higher values corresponding to transparent windows and lower values to windows with blinds shut.

The power provided by the heating system $P_{\rm h}(t)$ is a discrete valued function, which either vanishes when the heating is off or takes on its nominal heating power value, $P_{\rm h}(t) = P_{\rm h}^{\rm n}$, when the heating is on, i.e. $P_{\rm h}(t) = P_{\rm h}^{\rm n}\;s(t)$, with the switch function $s(t) = 1$ or 0 when the heating is on or off. Focusing on energy-efficient buildings, the heating systems we consider are heat pumps with a constant coefficient of performance (COP) equal to 3. Thus, the heating power $P_{\rm h}$ is three times larger than the consumed electric power. This COP is a reasonable approximation for modern ground source heat pumps.

III. Thermostatic Control vs. Demand Side Management.

A. Purely Thermostatic Control

A thermostat keeps a building's temperature within a certain range. In a conventional control scheme, heating is turned on as soon as the internal temperature of the building reaches a minimal temperature fixed by the user. It then keeps operating until the temperature reaches a maximal setpoint, at which time it is turned off. The building's temperature then falls down, leading to a new cycle. The minimal and maximal temperatures define a comfort temperature interval within

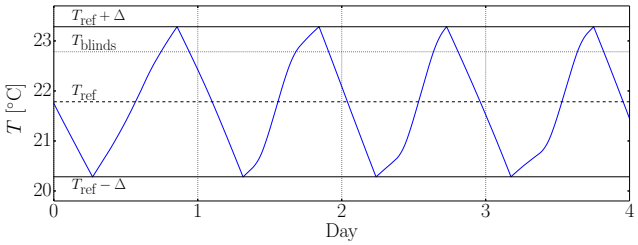

Fig. 2. Temperature profile inside a typical, energy-efficient building under thermostatic heating control, during four consecutive winter days in Sion, Switzerland. The first day is cloudy, while the next days are sunny, which manifests itself in a sharper temperature increase starting in the late morning, once solar radiations contribute to heating. Vertical dotted lines indicate midnight.

which the building's temperature should remain at all times, $T(t) \in [T_{\text{ref}} - \Delta, T_{\text{ref}} + \Delta]$, $\forall t$. It is defined by a reference temperature T_{ref} and a tolerance temperature interval 2Δ.

In addition to the heating system itself, solar radiation significantly contributes to heating. In order to maintain the temperature within the comfort bracket, solar radiation must therefore be controlled, which is achieved by shutting window blinds as soon as the temperature reaches the maximal temperature. This has the effect of strongly suppressing the solar gains and is modeled in (2) by a reduction of g. Blinds are opened back later, as the temperature falls below a given threshold T_{blinds}, usually above the minimal temperature. A resulting typical temperature profile over one sunny and one cloudy day is shown in Fig. 2.

B. Demand Side Management

As an alternative to the thermostat regulation protocol just outlined, we present a simple control scheme whose aim is to shift the electric consumption required for heating when it is more beneficial. Here "beneficial" can have one of many different meanings, including "financially beneficial" (minimizing electricity costs), "beneficial from the point of view of the DSO" (providing ancillary service, smoothing the load curve and so forth) or "beneficial for self-consumption" (allowing to consume locally as much as possible of a local production, for instance from photovoltaic panels). One of our goals is to try and suppress the large load oscillations emerging from the synchronization discussed in the introduction, however we stress that our approach is more generically applicable.

We first discretize time into intervals Δt ($t_i = i\,\Delta t$) and encode the information of when it is desirable to consume in a predetermined target consumption profile, $\{P_i\}$. This profile is chosen, for instance, according to one of the specific objectives we just listed. It is based on weather forecasts for the solar radiation $\{P_{\text{rad},i}\}$ and the outside temperature $\{T_{\text{ext},i}\}$, $i = 1, \dots N$, in a time-window corresponding to a receding time-horizon $N\Delta t$. How to effectively construct $\{P_i\}$ is discussed below. Here we always consider a time-horizon covering the next 24 hours. At each time step, loads adapt their instantaneous consumption, $\{E_i\}$ to try and minimize deviations from $\{P_i\}$ as measured by the variance

$$F\left(\{P_i\},\{E_i\}\right) = \sum_{i=1}^{N} (E_i - P_i)^2 \ . \tag{3}$$

It is instructive to first consider the case of ideally flexible loads. These are (i) fully flexible, in the sense that their daily consumption can be distributed over any time intervals of the day, and (ii) have a power consumption that can take any value between zero and their maximum rated power. Such loads have a consumption profile $\{E_i\}$ that is therefore allowed to vary freely, with the only constraint that their total daily consumption is fixed,

$$\sum_{i=1}^{N} E_i \ \Delta t = W_{\text{tot}} \, . \tag{4}$$

A closed form solution to the minimization of the function $F(\{P_i\},\{E_i\})$ under the constraint (4) is readily obtained using the method of Lagrange multipliers, yielding

$$\tilde{E}_i = \frac{W_{\text{tot}}}{N\Delta t} - \frac{1}{N}\sum_{l=1}^{N} P_l + P_i \, . \tag{5}$$

Here and in the following, $\tilde{E}$ denotes the solution which minimizes $F(\{P_i\},\{E_i\})$.

Having established analytically the solution which minimizes (3) in the case of an ideally flexible load, we next turn our attention to our central problem of TCL's. Clearly, a single heating system cannot be approximated as an ideally flexible load. The constraint of maintaining the house in the appropriate temperature interval only provides restricted flexibility (e.g. when the temperature is too low, the heating *must* be switched on). Furthermore, as discussed in Sec. II, conventional heating systems have a consumption that is either zero or equal to the nominal power. Yet, having an explicit analytical solution for ideally flexible loads, it is desirable to try and formulate our problem in a way that is as close as possible to that solution.

To turn thermostatically controlled heating systems into flexible loads we aggregate them. Instead of a single building we consider the total load of a large district with several hundreds of dwellings. Equations (3), (4) and (5) remain valid but the variables W_{tot}, $\{E_i\}$ and $\{P_i\}$ now represent aggregated quantities. The consumption at time i is then given by

$$E_i = \sum_k E_i^{(k)} \, , \tag{6}$$

where $E_i^{(k)}$ is the heating consumption of the k^{th} building, and the sum spans over the whole district. The objective consumption profile $\{P_i\}$ and the corresponding $\{\tilde{E}_i\}$ are generated by a central controller in charge of the full set of aggregated buildings. Aggregation increases the load flexibility because, first, if the number M of loads is large enough, one may legitimately hope that at any time there are enough individual loads ready to turn on or off – the aggregated load can be increased or decreased at any time to adapt to demand side management goals. Second, the aggregated consumption increases roughly in steps of $P^{\text{n}}_{\text{tot}}/M$, the aggregated nominal power $P^{\text{n}}_{\text{tot}}$ divided by the number M of individual loads, so

that the relative power consumption becomes effectively a continuous variable for $M \gg 1$.

Still, the operation of electric heating systems is required to keep the temperature inside each building within comfort temperature intervals $[T_{\rm ref}^{(k)} - \Delta^{(k)}, T_{\rm ref}^{(k)} + \Delta^{(k)}]$, $\forall k = 1, \dots M$, which differentiates them from ideally flexible loads. Thus we need to solve the following two major problems,

- How to estimate the total aggregated daily consumption required for heating and how to appropriately construct the target consumption profile?
- How does the central controller manage the individual heating systems so that the collective behavior matches the objective consumption profile in a non-disruptive way?

These questions are answered in the next section.

IV. DSM Coordination Algorithm.

Our algorithm is based on a central controller having two-way communication with each load. This guarantees that long-term DSM operation does not lead to temperature drifts beyond the comfort interval and that the synchronized behavior of heating systems during clear, cold days is suppressed. It is an important, yet future task of ours to try and implement a coordination algorithm with only one-way communication.

At every time step, the central controller estimates the energy consumption of the district for the receding time window covering the next 24 hours. This is made based on weather (temperature and solar radiation) forecasts and on the current energy content of the buildings. Let i_0 denote the considered time step. From (1), the estimate for $W_{\rm tot}$ at i_0 is obtained as

$$W_{{\rm tot},i_0} = \sum_k \sum_{i=i_0}^{i_0+N} \left[\kappa^{(k)} \left(-T_{{\rm ext},i} + T_{\rm ref}^{(k)}\right) - p_{{\rm rad},i}\, S^{(k)}\, g\right] \Delta t + \sum_k C^{(k)} \left[T_{\rm ref}^{(k)} - T_{i_0}^{(k)}\right], \tag{7}$$

where the sum over k runs over the whole district, with quantities corresponding to individual dwellings labeled by superscripts (k). The first term on the right-hand side of (7) corresponds to the energy needed to maintain every building at its reference temperature, given the external temperature forecast, minus the energy provided by solar radiation. The second term additionally takes into account the excess or deficit in stored thermal energy at the time of the estimate, compared to the energy stored at the reference temperature.

We note that the overall electric consumption is the sum of a flexible and a non-flexible contribution. The flexible consumption can be shifted in time, at least partially. The non-flexible consumption corresponds to all consumptions that either cannot be shifted, or whose flexibility is not used. In our case, the flexible consumption is that of the electric heating system, while the non-flexible consumption is the sum of the consumptions of all other domestic appliances (such as washing machines, fridges, stoves, ovens, etc.). The district's need for electric power is further quantified by the residual consumption R_i, which, as discussed above, we define as the sum of all non-flexible consumptions minus all non-flexible local productions. Our goal is to construct a coordination algorithm shifting the flexible consumption in such a way that the sum of the residual consumption and of the flexible consumption is smoother than without control. Thus, we want the electric heating system to function mostly in the valleys of the residual consumption. To achieve this, we chose the target consumption profile [the P_i's in (3)], as

$$P_i = \frac{W_{\rm tot}}{N\,\Delta t} - {\rm COP}\ R_i\,. \tag{8}$$

From (5) the optimal thermal consumption profile is given by

$$\tilde{E}_{i_0+i} = \left(\frac{W_{{\rm tot},i_0}}{N\,\Delta t} + \frac{1}{N}\sum_{l=1}^{N} {\rm COP}\ R_{i_0+l}\right) - {\rm COP}\ R_{i_0+i}\,. \tag{9}$$

Note that in (8) and (9) the residual consumption is an electric power and therefore it must be multiplied by the COP to obtain the corresponding thermal power. Obviously, the total electric consumption $\tilde{E}_{i_0+i}/{\rm COP} + R_{i_0+i}$ gives a smoothly varying function of time. It is given by the sum of the forecasted heating energy required for the next 24h, distributed uniformly over the corresponding N time intervals, plus the average of the residual consumption for the next 24h. The latter average renders $\tilde{E}_{i_0+i}/{\rm COP} + R_{i_0+i}$ smooth as a function of time.

With estimates for $W_{\rm tot}$ and $\{R_i\}$ in hand, the central controller generates the optimal consumption profile $\{\tilde{E}_i\}$ in the receding time window $i = i_0, \dots i_0 + N$, according to (9). The controller's task is then to adapt the district's actual load to $\{\tilde{E}_i\}$, under the end-use constraint that each bulding's inside temperature lies at any time within the comfort interval, $T_i^{(k)} \in [T_{\rm ref}^{(k)} - \Delta^{(k)}, T_{\rm ref}^{(k)} + \Delta^{(k)}]$. In our approach, this end-use constraint has priority over everything else. The procedure goes as follows. The central controller receives from each building

- the temperature $T_{i_0}^{(k)}$ of the building and its comfort temperature-interval, and
- the nominal power $P_{\rm h}^{{\rm n},(k)}$ and the state $s_{i_0}^{(k)}$ of each heating system.

The priority list is then constructed by ranking the houses according to a priority index

$$\eta_{i_0}^{(k)} \equiv \frac{T_{i_0}^{(k)} - \left(T_{{\rm ref},i_0}^{(k)} - \Delta^{(k)}\right)}{2\,\Delta^{(k)}} \in [0,1]\,, \tag{10}$$

encoding how close the $k^{\rm th}$ house is to the minimal ($\eta_{i_0}^{(k)}$ small) or to the maximal temperature ($\eta_{i_0}^{(k)}$ closer to one).

The controller next computes the district's instantaneous consumption,

$$E_{i_0}^{\rm inst} = \sum_k P_{\rm h}^{{\rm n},(k)}\ s_{i_0}^{(k)}\,, \tag{11}$$

which is the heating load that the district would have with purely thermostatic control. The controller then compares $E_i^{\rm inst}$ to $\tilde{E}_i$. If $E_i^{\rm inst} < \tilde{E}_i$, it instructs the coldest buildings, starting with those with lowest $\eta_{i_0}^{(k)}$, to turn on their heating systems until the actual load reaches $\tilde{E}_i$. If $E_i^{\rm inst} > \tilde{E}_i$ on the other hand, it instructs the warmest buildings, starting with those with highest $\eta_{i_0}^{(k)}$, to turn off their heating system. Implemented blindly, this procedure could lead either to violations of the

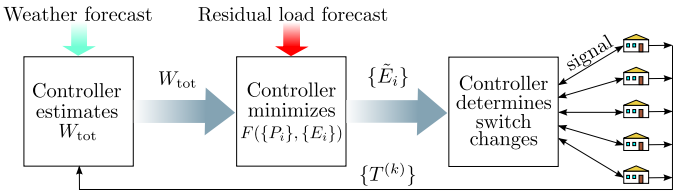

Fig. 3. Schematic representation of the control loop.

temperature constraint $T_i^{(k)} \in [T_{\text{ref}}^{(k)} - \Delta^{(k)}, T_{\text{ref}}^{(k)} + \Delta^{(k)}]$ or to frequent switchings of the heating systems (the number of which determines the lifetime of a heat pump) or both. To avoid that, our algorithm finally imposes that the central controller can command heating systems to turn off (resp. on) only in buildings with temperatures $T \in [T_{\text{ref}} - 0.9\ \Delta, T_{\text{ref}} + \Delta]$ (resp. $T \in [T_{\text{ref}} - \Delta, T_{\text{ref}} + 0.9\ \Delta]$) – when temperatures are outside these intervals, thermostat rules apply. This core part of our control algorithm takes into account both the "willingness" [quantified in terms of the priority index (10)] and the "availability" (corresponding to which pumps are available to change their operating state) of the TCL to participate in the DSM coordination.

Once the switching commands are sent the controller lets the district evolve according to (1) during one time step Δt. The new building temperatures are then transmitted back to the central controller, which closes the control loop. The next step is then initiated with a new estimate of W_{tot} and of $\{R_i\}$ for the next 24h, a new priority list is constructed and the procedure just outlined is implemented again. In our receding horizon approach, new estimates of W_{tot} and $\{R_i\}$ and a new optimization of the consumption profile are performed at each time step. We found that this allows to correct forecast errors rapidly. The control loop is illustrated in Fig. 3.

V. Simulation Parameters and Results.

A. Building parameters

In all our simulations, we consider a district consisting of 1000 individual houses, modeled by 1000 copies of (1) discretized in time steps $\Delta t = 1$ min. The parameters we use in these differential equations are different for each house and distributed as follows. The thermal capacity is uniformly distributed in the interval

$$C \in [13, 27]\ \text{kWh/K}\,, \tag{12}$$

which is a common range for detached European houses with a floor surface ranging from 100 to 200 m^2. We take the effective thermal conductivity κ uniformly distributed in the interval

$$\kappa \in [200, 400]\ \text{W/K}\,, \tag{13}$$

which, for the particular case of Switzerland, includes both recent energy efficient houses (lower range, i.e. $\kappa \in [200, 300]$ W/K) as well as older houses as commonly built in the early 90's (upper range, $\kappa \in [300, 400]$ W/K) [6].

We calibrate the nominal heating power of each heat pump as

$$P_{\text{h}}^{\text{n}} = \kappa \cdot 30\,\text{K}\,, \tag{14}$$

so that the pump can provide sufficient heating power to maintain the houses at $T = 20$°C against an external temperature of $T_{\text{ext}} = -10$°C.

According to (13) and (14), the nominal thermal powers of the heating systems are uniformly distributed in the interval

$$P_{\text{h}}^{\text{n}} \in [6, 12]\ \text{kW}\,. \tag{15}$$

The corresponding electric consumption is obtained by dividing (15) by the COP assumed to be constant, COP = 3.

The houses in our district may have different orientations and are thus subject to different solar gains. We take this into account by distributing their effective south facing window surface uniformly in the interval

$$S \in [10, 20]\ \text{m}^2\,. \tag{16}$$

Furthermore, the transmission coefficient of the windows is either $g = 0.6$ or $g = 0.12$ when the blinds are up or down respectively. Blinds are closed at the maximal tolerated temperature, $T = T_{\text{ref}} + \Delta$, and are opened back at $T_{\text{blinds}} = T_{\text{ref}} + (2/3)\ \Delta$. The comfort interval parameters T_{ref} and Δ reflect end-user habits and preferences. They are uniformly distributed as

$$T_{\text{ref}} \in [21, 23]\ ^\circ\text{C}\,, \quad \Delta = 1.5\ ^\circ\text{C}\,. \tag{17}$$

B. Non-flexible domestic appliances

The electrical load of the district we consider is the sum of the consumption of domestic appliances and of the electric heating systems. DSM coordinates only the latter as domestic appliances are considered non-flexible in this work. We generate load profiles from domestic appliances with the BEHAVSIM simulation software [13]. The resulting load for all domestic appliances in our district is shown in Fig. 4 a). The non-flexible load displays a characteristic double peak structure with peaks at noon and in the early evening. A smaller peak is also present in the early morning of working weekdays. There is a $\sim$ 1.3 kW daily excursion per house between the peak consumption of 1.5 kW and the base load of 0.2 kW. Our task is to adapt the electric heating consumption to obtain a total load curve that is as smooth as possible.

In investigations of districts with their own, local PV production, we try to additionally consume locally as much of the PV production as possible. The quantity of interest in this case is the residual consumption, defined above in Section IV. The profile of the residual consumption for a district with 1000 houses and 5000 m^2 of solar panels is shown in Fig. 6 a). Compared to the consumption of domestic appliances shown in Fig. 4 a) we see that, on sunny days, the PV production erases the noon consumption peak so that we are left with a single, early evening peak above a fluctuating background at around 0.3 kW per house on average. Note that the residual consumption may be negative at times of relatively low consumption and large PV production, indicating a need to either consume, store or export part of the local PV production.

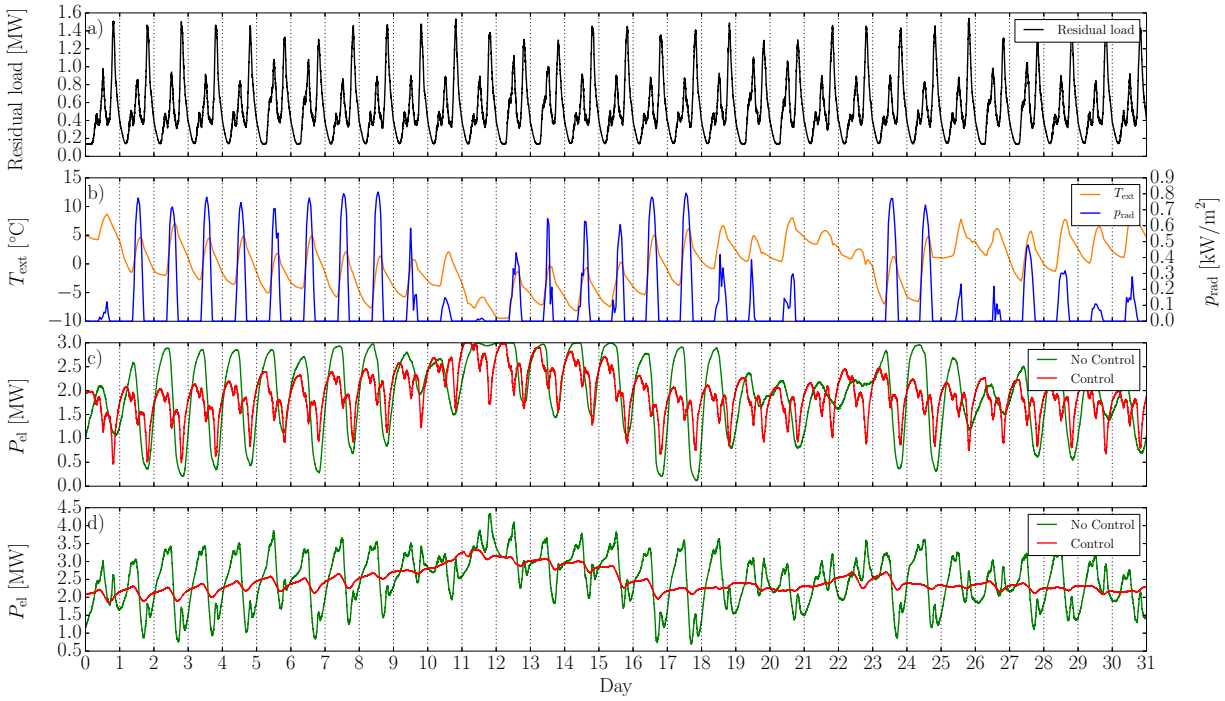

Fig. 4. (Color Online) Time series for electrical consumptions and weather conditions for a winter month in Sion, Switzerland. Consumptions correspond to aggregated values for a district of 1000 individual houses and vertical dotted lines correspond to midnight. Panel a): Residual load from all domestic appliances (there is no PV production). Panel b): External temperature (orange) and solar radiation (blue) data. Panel c): Total electrical consumption of the heating systems with and without control. Panel d): Total load given by the sum of the heating consumption and of the residual load. In panels c) and d), green curves correspond to purely thermostatic control, while red curves are obtained with DSM coordination.

C. Meteorological data

Time series for the external temperature $T_{\text{ext}}(t)$ and solar radiation data $p_{\text{rad}}(t)$ are obtained from the software Meteonorm, which gives either true (recorded) or interpolated data[1]. Below, we discuss sequentially different situations of a typical winter month in Sion, Switzerland, both with and without photovoltaic production that needs to be self-consumed. We performed other investigations, not shown here, for different weather conditions corresponding to typical winter conditions for the cities of London, Milan and Paris.

D. District without local production

For a district without local production, the residual consumption is given by the load of the domestic appliances. An example of such residual consumption is shown in Fig. 4 a). It corresponds to 1000 individual houses in January in Sion, Switzerland, for which temperature and solar radiation time series are shown in Fig. 4 b). Additionally to daily modulations, we observe longer-term variations of the temperature with the coldest day of the month being cloudy without solar radiation and with temperatures almost reaching -10°C. Without PV production, the solar radiation influences our results only via the radiation gains defined in (1) and (2).

Results for the electric heating and total loads, with and without DSM coordination are shown in the bottom panels c) and d) of Fig. 4. It is clearly seen in Fig. 4 c) that, without DSM coordination, the heat pumps tend to synchronize and the heating consumption correlates with the external weather conditions. The trend is especially visible on clear, cold days, when solar radiation provides enough heating power [the last term in (1)] so that no electric heating is necessary from midday until the late afternoon. The temperature drops fast, however, when the sun sets, at which time almost all heat pumps switch on (signaled by a total consumption reaching ~ 3.0 MW) and, because the night is cold, they stay on until the next day. If that day is also clear, a new cycle starts and the pumps are almost perfectly synchronized. This behavior is observed almost throughout the month, with fluctuations being damped, but not suppressed, on cloudy days with little or no solar radiation.

Numerical simulations performed using cloudier weather conditions in London, Milan and Paris (not shown) corroborate our finding that, without control, large load fluctuations already emerge after a single sunny day and reach their maximal amplitude of 2.5 kW/house after two consecutive clear days. We conclude that the onset of synchronization of heat pumps is fast in energy-efficient buildings, and mostly depends on solar radiation, external temperature being a subdominant factor.

The synchronization of the heat pumps is also reflected in the total load shown in Fig. 4 d), which exhibits daily fluctuations reaching 3 MW for our set of 1000 houses. Striking in Fig. 4 d) is that the total load on the distribution network exhibits sharp ramp-down of more than 2 MW in just two hours or less during more than ten days of the month.

[1]For more details we refer the reader to *meteonorm.com*.

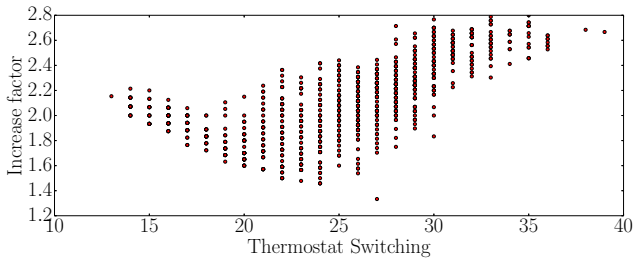

Fig. 5. Increase in the number of heat pump switchings resulting from DSM for the simulation results shown in Fig. 4. Horizontal axis: monthly number of heat pump switchings without DSM. Vertical axis: multiplicative factor of the number of switchings with DSM.

Such abrupt variations need to be smoothed to avoid potential service disruptions. Achieving this is a priori a hard task: it requires to operate a significant fraction of heat pumps at times of higher solar gains and to turn them off during cold night hours.

Fig. 4 c) and d) show how the DSM coordination algorithm described in Section IV manages to smooth the total load of our district. The heating consumption in Fig. 4 c) is clearly anticorrelated with the load from the domestic appliances. The result is that the total load, shown in Fig. 4 d), becomes remarkably smooth. With DSM, the amplitude of daily fluctuations do not exceed 0.5 MW which is about five times less than the amplitude of 2.5 MW under thermostatic control only.

Any DSM protocol such as ours should have almost no negative impact on end-use performance – in our case, it should cause no violation of the comfort temperature window set by the end users, it should not generate frequent switching on and off of the electric heating systems, and it should not significantly increase the total electric consumption. For the results presented in Fig. 4 c) and d), we have that $T_i^{(k)} \in [T_{\text{ref}}^{(k)} - \Delta^{(k)}, T_{\text{ref}}^{(k)} + \Delta^{(k)}]$ for all houses at any time of the month. Additionally, we find that the total monthly consumption with DSM is few percent smaller than without DSM. Finally, Fig. 5 shows that, with DSM, the number of switchings of the heat pumps increases only by a factor of 1.5 to 3, which is tolerable.

For other weather conditions not shown here (London, Milan and Paris), we find that our DSM protocol performs as well as it does for Sion. It is non-disruptive in the sense discussed above, and it reduces the daily excursions of the total load below 0.5 MW.

E. Non-flexible domestic appliances and local photovoltaic production

We next consider a district with a moderate local PV production corresponding to a total of 5000 m^2 of PV panels for our 1000 houses. We generate the PV production time series by multiplying the solar radiation data on a south facing, 40° degrees inclined surface by the total surface of PV panels, times an efficiency coefficient of 15%. The latter corresponds to standard commercial PV panels. Our goal is now not only to smoothen the load curve but to do so while simultaneously consuming as much as possible of the PV production. This is not a trivial task – solar panels produce the most when solar gains are maximal, i.e. when electric heating systems would rather switch off. We show that our DSM protocol can still achieve this goal, at least for not too large PV penetration.

The residual load is now given by the domestic appliances' consumption minus the PV production. The residual consumption, shown in Fig. 6 a), loses its noon peak, being counterbalanced by the PV production. As a matter of fact the chosen penetration of PV produces about the noon consumption of electric appliances. Meteorological conditions are the same as in the previous example and are shown in Fig. 4 b).

The aggregated heating consumption of the 1000 heat pumps is presented in Fig. 6 b) for both coordinated and uncoordinated operation. In the uncoordinated case the results are the same as those presented in Fig. 4 c) – they do not depend on PV production. In contrast, the heating consumption in the coordinated case is now higher at noon, to compensate the PV production. Fig. 6 c) finally presents the total load on the distribution grid, which is about as smooth as without PV production. We conclude that our algorithm is able to smooth the load of a relatively large district while simultaneously absorbing a local PV production, even with large solar radiation power – despite the fact that the latter simultaneously reduces the need for heating and increases PV production.

We note that, with PV production, our coordination protocol still meets our requirement of being non-disruptive: we observe no violation of the comfort temperature interval, nor dramatic increase in the number of heat pump switches. We even find a small, though not statistically significant, reduction of the total consumption with DSM coordination compared to the case with purely thermostatic control.

VI. Conclusion.

We have presented a centralized DSM scheme to control the heating consumption of a relatively large district of residential buildings equipped with heat pumps. Our goal was to generate a load curve which is smoother than without control to provide a service to the DSO.

We first found that, in energy-efficient buildings, heat pumps operated by purely thermostatic control quickly synchronize, and that solar heat gains are the dominant factor inducing this synchronization. In clear winter days with significant solar gains, we found that more than 80% of the heating systems turn on and off simultaneously, which leads to massive load modulations and sharp ramp-ups and -downs of more than 2 MW in just two hours for 1000 houses. This undesirable synchronization is likely to become more pronounced as buildings become more and more energy efficient.

We have constructed a DSM algorithm that strongly suppresses these large load fluctuations and demonstrated the load-shifting potential of DSM: for 1000 houses, load fluctuation amplitudes have been damped from 2.5MW down to 0.5MW. We furthermore showed that the same control scheme is able to additionally absorb a local PV production, even though the latter is produced at the same time solar gains are maximal and heat pumps have a natural tendency to switch off. We demonstrated that our algorithm is robust in that it

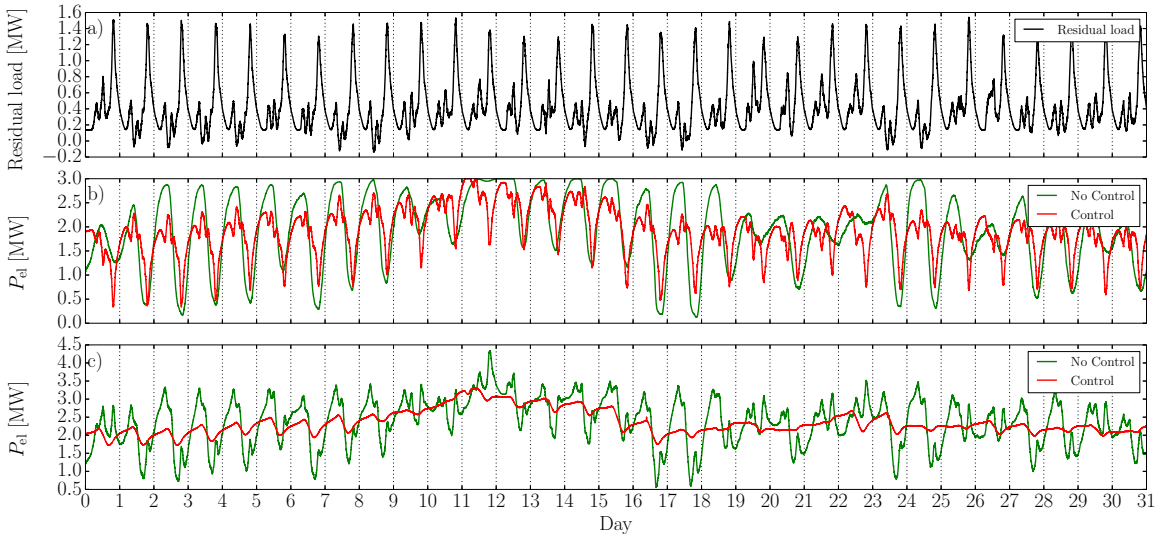

Fig. 6. (Color Online) Time series for electrical consumptions for a winter month in Sion, Switzerland. Consumptions correspond to aggregated values for a district of 1000 individual houses and vertical dotted lines correspond to midnight. Panel a): Residual load from all domestic appliances minus a local PV production from 5000 m^2 of solar panels. Panel b): Total electrical consumption of the heating systems with and without control. Panel c): Total load given by the sum of the heating consumption and of the residual load. In panels b) and c), green curves correspond to purely thermostatic control, while red curves are obtained with DSM coordination.

works well in different geographical regions with different meteorological conditions. In all our investigations we finally found that our DSM scheme is non disruptive in the sense that: i) comfort temperature intervals set by the users are not violated, ii) the overall consumption never exceeds that of the uncoordinated case and iii) the increase in heat pump switchings remains reasonable.

Our work successfully demonstrated the large potential for DSM of TCLs over long periods of time. Our proof-of-principle algorithm relies on a two-way communication protocol between a central controller and local load controllers. We see this as the main shortcoming in our approach and future works should attempt to adapt this idealized control scheme to one-way communication. To allow the self-consumption of larger PV injections, for which the flexibility limits of the district are reached, our algorithm could be extended either by allowing small, temporary violations of the temperature comfort intervals or by taking local storage capabilities into account.

Acknowledgment

This work has been supported by the Swiss National Science Foundation under an AP Energy Grant and by the HES-SO under the I1 funding scheme. The authors thank G. Basso, P. Ferrez, P.-O. Moix, G.-A. Morand and P. Roduit for useful discussions on the research reported here and especially D. Gabioud for providing the starting idea that initiated this project.

References

[1] D. Callaway and I. Hiskens, "Achieving controllability of electric loads," in *Proceedings of the IEEE*, vol. 99, no. 1, Jan 2011, pp. 184–199.

[2] J. L. Mathieu, M. Dyson, and D. S. Callaway, "Using residential electric loads for fast demand response: The potential resource and revenues, the costs, and policy recommendations," in *Proceedings of the ACEEE Summer Study on Buildings, Pacific Grove, CA*, Aug 2012, pp. 189–203.

[3] M. Kamgarpour, C. Ellen, S. Soudjani, S. Gerwinn, J. Mathieu, N. Mullner, A. Abate, D. Callaway, M. Franzle, and J. Lygeros, "Modeling options for demand side participation of thermostatically controlled loads," in *Bulk Power System Dynamics and Control - IX Optimization, Security and Control of the Emerging Power Grid, IREP Symposium*, Aug 2013, pp. 1–15.

[4] S. Koch, D. Meier, M. Zima, M. Wiederkehr, and G. Andersson, "An active coordination approach for thermal household appliances; local communication and calculation tasks in the household," in *PowerTech, IEEE Bucharest*, June 2009, pp. 1–8.

[5] N. Lu and Y. Zhang, "Design considerations of a centralized load controller using thermostatically controlled appliances for continuous regulation reserves," *IEEE Transactions on Smart Grid*, vol. 4, no. 2, pp. 914–921, June 2013.

[6] G. Maître, G. Basso, C. Steiner, D. Gabioud, and P. Roduit, "Distributed grid storage by ordinary house heating variations: A swiss case study," in *Euromicro Conference on Digital System Design*, Aug 2015, pp. 241–249.

[7] K. Christakou, D.-C. Tomozei, J.-Y. Le Boudec, and M. Paolone, "Gecn: Primary voltage control for active distribution networks via real-time demand-response," *IEEE Transactions on Smart Grid*, vol. 5, no. 2, pp. 622–631, March 2014.

[8] Y. Mu, J. Wu, J. Ekanayake, N. Jenkins, and H. Jia, "Primary frequency response from electric vehicles in the great britain power system," *IEEE Transactions on Smart Grid*, vol. 4, no. 2, pp. 1142–1150, June 2013.

[9] K. Samarakoon, J. Ekanayake, and N. Jenkins, "Investigation of domestic load control to provide primary frequency response using smart meters," *IEEE Transactions on Smart Grid*, vol. 3, no. 1, pp. 282–292, 2012.

[10] K. Dehghanpour and S. Afsharnia, "Electrical demand side contribution to frequency control in power systems: a review on technical aspects," *Renewable and Sustainable Energy Reviews*, vol. 41, pp. 1267 – 1276, 2015.

[11] S. Ihara and F. Schweppe, "Physically based modeling of cold load pickup," *IEEE Transactions on Power Apparatus and Systems*, vol. PAS-100, no. 9, pp. 4142–4150, Sept 1981.

[12] S. Kundu, N. Sinitsyn, S. Backhaus, and I. Hiskens, "Modeling and control of thermostatically controlled loads," in *17th Power Systems Computation Conference (PSCC), Stockholm, Sweden*, August 2011.

[13] P. Ferrez and P. Roduit, "Non-intrusive appliance load curve disaggregation for service development," in *IEEE International Energy Conference (ENERGYCON)*, May 2014, pp. 813–820.